Supplemental Materials

Molecular Biology of the Cell

Wullkopf et al.

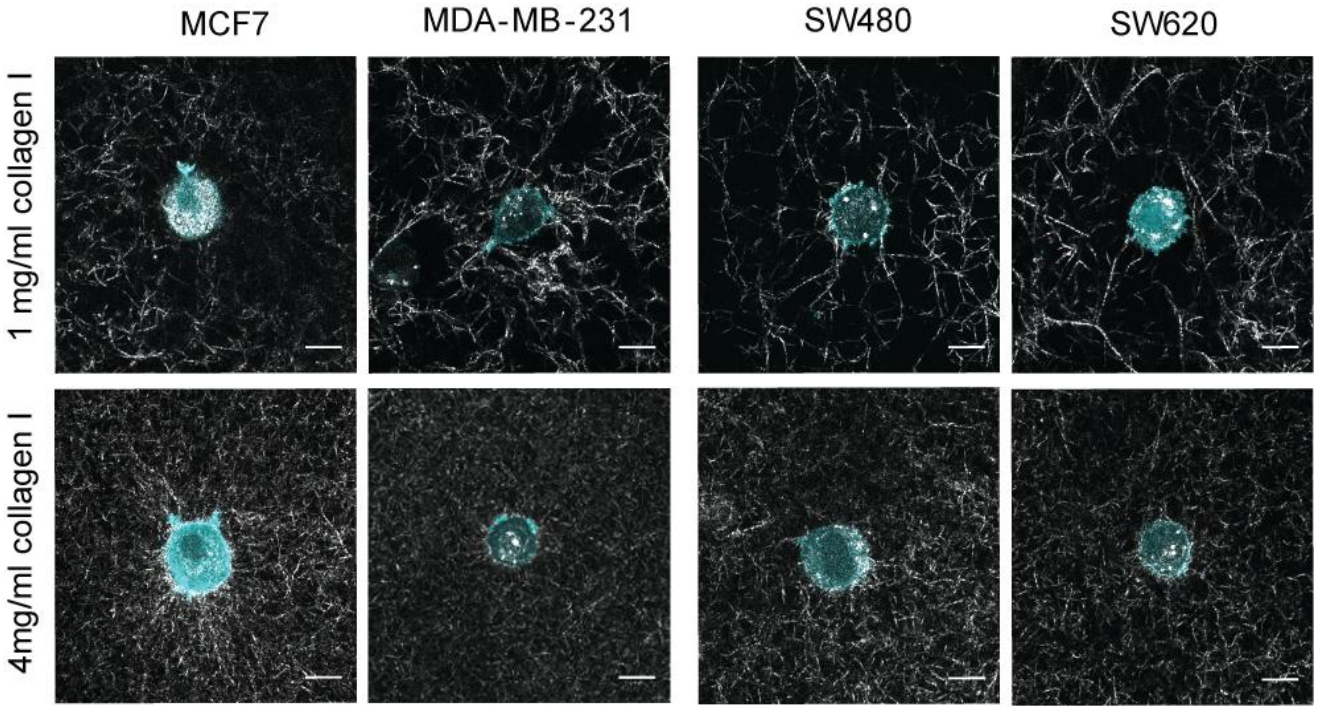

Supplemental Figure S1.

Three dimensional collagen culture of cancer cells. Representative pictures of mEmerald-lifeAct-7-labeled MDA-MB-231 and MCF7 breast cancer as well as SW620 and SW480 colorectal cancer cells cultured in matrices of 1 or 4 mg/ml rat-tail collagen I. Scale bars depict 10µm.

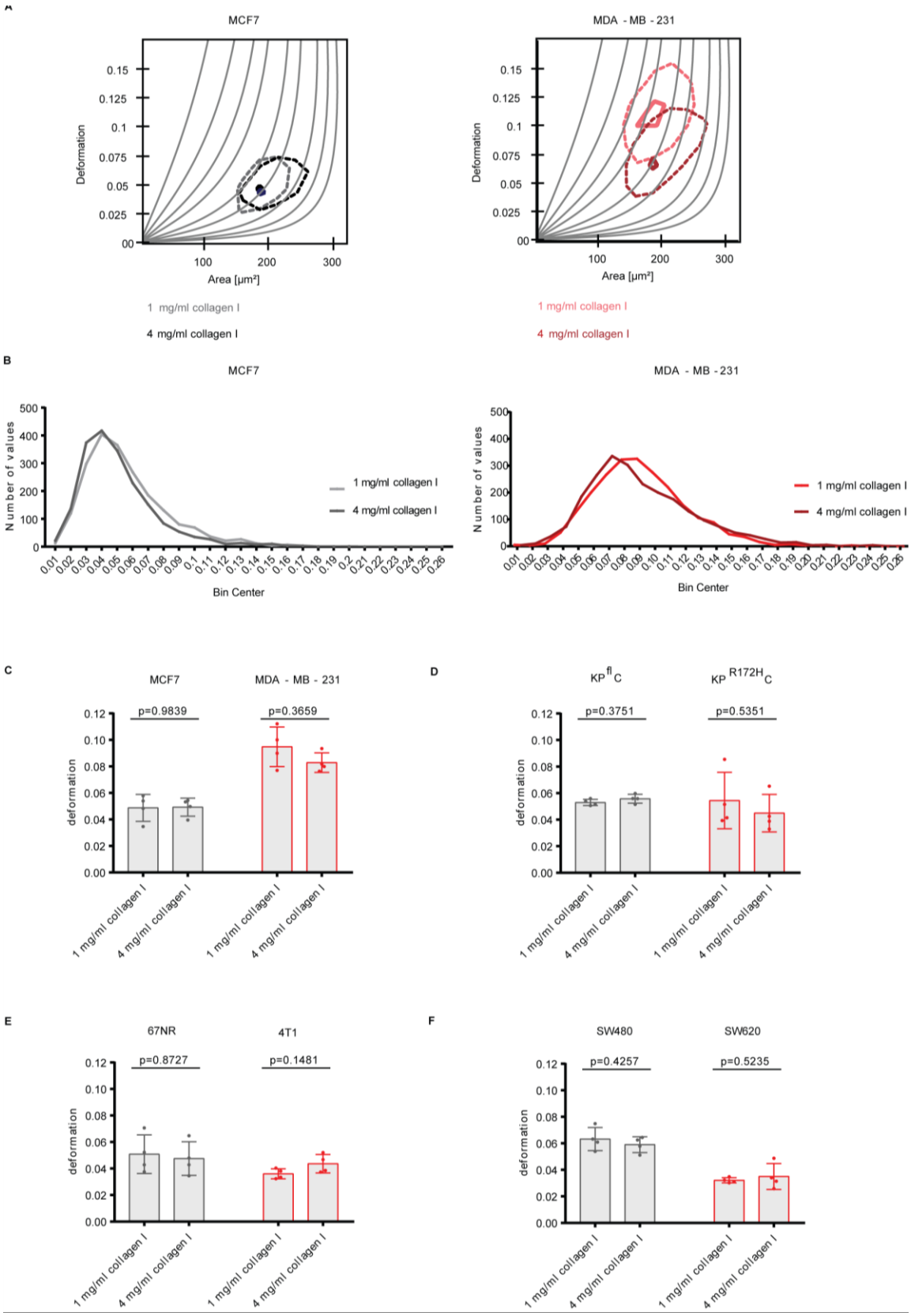
A
MCF7
MDA - MB - 231
Deformation
Area [µm²]
1 mg/ml collagen I
4 mg/ml collagen I
B
MCF7
MDA - MB - 231
Number of values
Bin Center
1 mg/ml collagen I
4 mg/ml collagen I
C
MCF7
MDA - MB - 231
p=0.9839
p=0.3659
deformation
D
KP fl C
KP R172H C
p=0.3751
p=0.5351
E
67NR
4T1
p=0.8727
p=0.1481
F
SW480
SW620
p=0.4257
p=0.5235

Supplemental Figure S2.
Deformability of cancer cells cultured on matrices of different collagen I concentration. (**A**) Exemplary scatter plot of deformability and cell size of non-invasive MCF7 and invasive MDA-MB-231 cells after 24h culture on matrices of 1 or 4 mg/ml collagen I. (**B**) Histogram of the overall distribution of deformation values of non-invasive MCF7 and invasive MDA-MB-231 cells after 24h culture on matrices of 1 or 4 mg/ml collagen I (n=2000). (**C**)-(**F**) Quantification of the median deformability of human breast cancer cell lines MCF7 and MDA-MB-231 (**C**), pancreatic cancer cell lines $KP^{fl}C$ and $KP^{R172H}C$ (**D**), mouse breast cancer cell lines 67NR and 4T1 (**E**) and colorectal cancer cell lines SW480 and SW620 (**F**) after 24h of culture on matrices of 1 or 4 mg/ml collagen I. Non-invasive cell lines are displayed left and invasive lines on the right side of each graph. Error bars depict SD, n=4. p-values are derived from a paired students t-test.

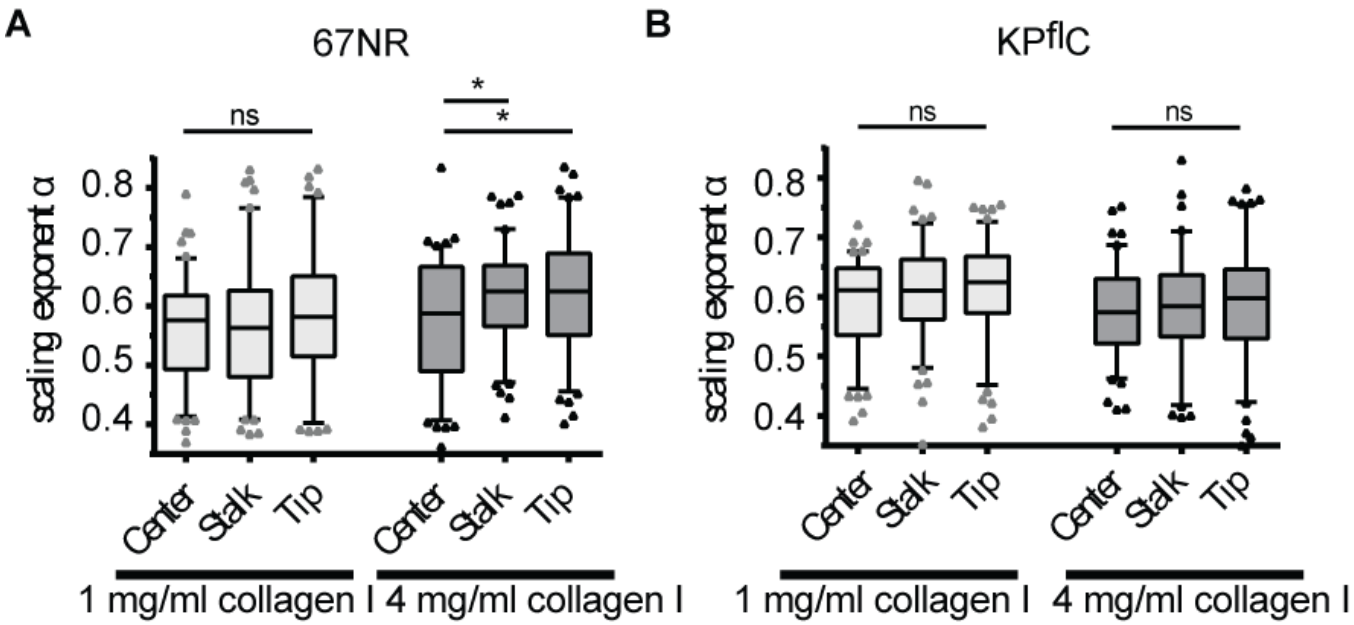

Supplemental Figure S3.
Characterization of the intracellular viscoelasticity of cancer cells of non-invasive status in different positions of a spheroid. (**A**) - (**B**) Assessment of the scaling exponent, α, characterizing intracellular lipid granule diffusion in 67NR (**A**) and $KP^{fl}C$ (**B**) either in the center, in the stalk or at the tip of an invading branch of a spheroid embedded in matrices of 1 or 4 mg/ml collagen I. * $p<0.05$ in a Kruskal Wallis test with Dunn's multiple comparison.

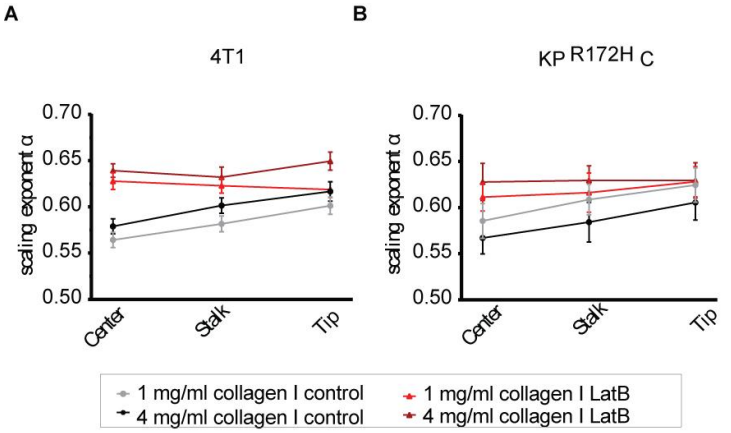
A
4T1
B
KP R172H C
0.70
0.65
0.60
0.55
0.50
scaling exponent α
Center
Stalk
Tip
1 mg/ml collagen I control
4 mg/ml collagen I control
1 mg/ml collagen I LatB
4 mg/ml collagen I LatB

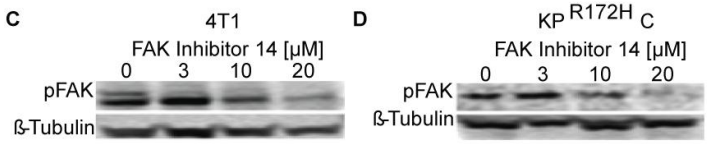
C
4T1
FAK Inhibitor 14 [μM]
0
3
10
20
pFAK
ß-Tubulin
D
KP R172H C
FAK Inhibitor 14 [μM]
0
3
10
20
pFAK
ß-Tubulin

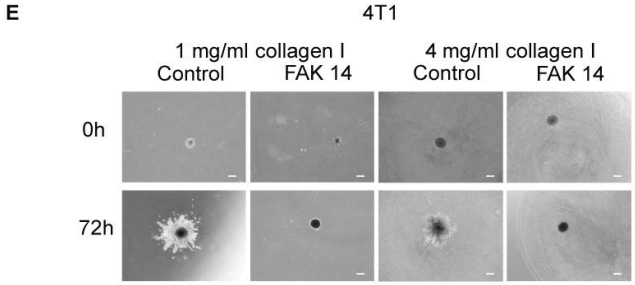
E
4T1
1 mg/ml collagen I
Control
FAK 14
4 mg/ml collagen I
Control
FAK 14
0h
72h

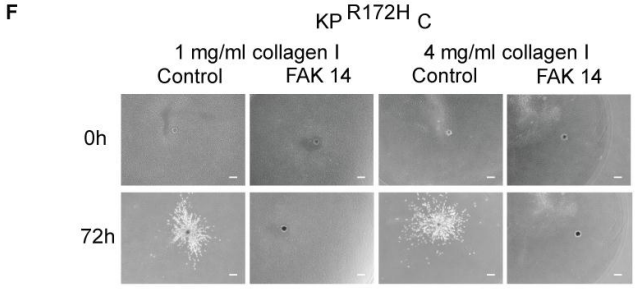
F
KP R172H C
1 mg/ml collagen I
Control
FAK 14
4 mg/ml collagen I
Control
FAK 14
0h
72h

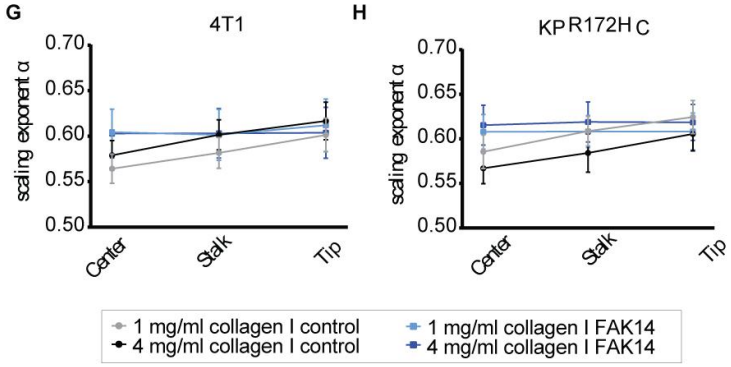
G
4T1
H
KP R172H C
0.70
0.65
0.60
0.55
0.50
scaling exponent α
Center
Stalk
Tip
1 mg/ml collagen I control
4 mg/ml collagen I control
1 mg/ml collagen I FAK14
4 mg/ml collagen I FAK14

Supplemental Figure S4.
Targeting components of the force sensing machinery levels out mechanical differences of invasive and non-invasive cells. (**A**)-(**B**) Comparison of the mean scaling exponent of trapped lipid granules in 4T1 (**A**) and $KP^{R172H}C$ (**B**) cells in different positions of the spheroid after 72h of invasion intro collagen matrices of 1 and 4 mg/ml. While control cells show an increasing viscosity with their invasive phenotype (grey and black line), LatB treated cells show a higher and rather constant scaling exponent in all position of the sphere (light and dark red line). (**C)-(D**) Immunoblotting of pFAK in 4T1 (**C**) and $KP^{R172H}C$ (**D**) cells treated with 0, 3, 10, 20 µM of FAK 14. β-Tubulin is used as loading control. (**E**)-(**F**) Representative images of the invasion of control and FAK 14 (20µM) treated 4T1 (**E**) and $KP^{R172H}C$ (**F**) cancer cell spheroids into collagen matrices. The scale bars depict 200µm (**G)-(H**) Comparison of the scaling exponent, α, characterizing the viscoelasticity of 4T1 (**G**) and $KP^{R172H}C$ (**H**) cells in different positions of control (grey and black line) and FAK 14-treated (light and dark blue line) spheroid. Error bars depict SEM. The viscoelasticity of LatB and FAK14 treated cells in different positions of the spheres and the different matrices was compared in a Kruskal Wallis test with Dunn's multiple comparison.

Supplemental Table 1.
Overview of the scaling exponent in control, LatB and FAK14 treated 4T1 and $KP^{R172H}C$ spheroids. Data shown as mean ± SD, n=100.

4T1	**1 mg/ml collagen I**			**4 mg/ml collagen I**		
	Center	**Stalk**	**Tip**	**Center**	**Stalk**	**Tip**
Control	0.56 ± 0.08	0.58 ± 0.09	0.60 ± 0.09	0.58 ± 0.08	0.60 ± 0.08	0.62 ± 0.10
LatB	0.63 ± 0.09	0.62 ± 0.08	0.62 ± 0.09	0.64 ± 0.07	0.63 ± 0.10	0.65 ± 0.10
FAK 14	0.60 ± 0.13	0.60 ± 0.13	0.61 ± 0.14	0.60 ± 0.13	0.60 ± 0.14	0.60 ± 0.14
$KP^{R172H}C$	**1 mg/ml collagen I**			**4 mg/ml collagen I**		
	Center	**Stalk**	**Tip**	**Center**	**Stalk**	**Tip**
Control	0.59 ± 0.10	0.61 ± 0.08	0.62 ± 0.09	0.57 ± 0.09	0.58 ± 0.11	0.61 ± 0.09
LatB	0.61 ± 0.07	0.62 ± 0.10	0.63 ± 0.08	0.63 ± 0.10	0.63 ± 0.08	0.63± 0.09
FAK 14	0.61 ± 0.10	0.61 ± 0.09	0.61 ± 0.10	0.62 ± 0.11	0.62 ± 0.11	0.62 ± 0.10